energies

MDPI

Article

Performance Evaluation of Solar-Powered Atmospheric Water Harvesting Using Different Glazing Materials in the Tropical Built Environment: An Experimental Study

Husam S. Al-Duais [1], Muhammad Azzam Ismail [1,*], Zakaria Alcheikh Mahmoud Awad [2] and Karam M. Al-Obaidi [3,*]

[1] Department of Architecture, Faculty of Built Environment, Universiti Malaya, Kuala Lumpur 50603, Malaysia; haldoais@yahoo.com
[2] Department of Urban and Regional Planning, Faculty of Built Environment, Universiti Malaya, Kuala Lumpur 50603, Malaysia; zakaria2009@um.edu.my
[3] Department of the Natural and Built Environment, College of Social Sciences and Arts, Sheffield Hallam University, Sheffield S1 1WB, UK
* Correspondence: ma.ismail@um.edu.my (M.A.I.); k.al-obaidi@shu.ac.uk (K.M.A.-O.)

Abstract: Water scarcity is a global issue, and its severity is expected to worsen in the near future, prompting further efforts to find new sources of freshwater. Solar-Powered Atmospheric Water Harvesting (SPAWH) is a promising passive approach for atmospheric water generation. This study aims to examine the thermal performance of different glazing materials and water production in SPAWH. The research consists of two phases: a laboratory test of various glazing materials and an experimental study to assess system efficiency in producing water in the tropics. The preliminary results indicated that glass demonstrated better thermal performance than acrylic in the lab, with higher thermal conductivity and less heat loss. The experimental findings showed that the maximum water produced by the proposed SPAWH (60 cm length, 60 cm width and 30 cm height) placed on a 30° tilt angle using glass (3 mm) and acrylic (3 mm) was 0.61 L/m^2/day and 0.44 L/m^2/day, respectively. The cost analysis revealed that produced water costs $0.18/kg for glass and $0.40/kg for acrylic, respectively. Atmospheric water could be harvested using SPAWH in the tropics, which would help to provide new opportunities for sustainable water supplies and development in these regions.

Keywords: water generation; atmospheric water harvesting; desiccant materials; solar still; tropics

Citation: Al-Duais, H.S.; Ismail, M.A.; Awad, Z.A.M.; Al-Obaidi, K.M. Performance Evaluation of Solar-Powered Atmospheric Water Harvesting Using Different Glazing Materials in the Tropical Built Environment: An Experimental Study. *Energies* **2022**, *15*, 3026. https://doi.org/10.3390/en15093026

Academic Editor: Pouya Ifaei

Received: 26 March 2022
Accepted: 13 April 2022
Published: 21 April 2022

1. Introduction

Climate change affects water resources in complex ways; it changes weather patterns, unpredictably affects water availability and would contaminate water supplies. By 2100, the world population is expected to reach nearly 10.9 billion [1]. Such population growth will add massive pressure on drinking water supplies [2]. In addition, Shiklomanov indicated in a study entitled water in crisis: a guide to the world's freshwater resources that there is only 2.5% freshwater on the planet, while the rest is saline water [3]. The statistics showed that the current 2.5% of freshwater is categorized into 30% groundwater and 70% in the form of ice and snow [4,5]. As a result, only less than 1% of freshwater is available for human consumption.

Globally, the distribution of available water resources is not responding to the population's actual needs and activities. Many countries possess plenty of freshwater resources while they are insufficient in other countries. Even though some of those countries have sufficient water, such as Southeast Asia countries, the dynamic urbanization and climate change negatively affect the availability of water resources. Many polluting materials are discharged every year into many rivers in Southeast Asia countries. Simultaneously, this region is vulnerable to a variety of hydro-meteorological hazards, many of which are

likely to worsen as a result of climate change. Lorenzo and Kinzig [6] asserted that severe disasters, such as flooding, can have an immediate impact on water quality and cause long-term infrastructure damage in many tropical countries.

Atmospheric water harvesting (AWH) is considered an effective technique to increase water production [7,8]. Beysens and Milimouk [9] pointed out that the atmosphere contains 12,900 km^3 of freshwater, where 98% is water vapor, and only 2% occurs in the form of clouds. If we consider a volume of humid air as a thermodynamic system, converting water from vapor to liquid requires a decrease in entropy and enthalpy. Hence, energy must be removed from the system. Latent water vapor energy can be transferred when the ambient temperature is less than the dew point temperature, which occurs in only two settings. The first scenario is to position the system near a source of cold with a temperature lower than the dew point, such as the case with dew condensation and direct cooling systems. The second scenario is when the system pressure and the dew point temperatures increase above the ambient temperature similar to sorption/desorption systems [10].

The fundamental advantage of adsorption systems is the ability to generate energy from low-temperature heat sources. Generally, low-cost and environmentally friendly resources are used, such as solar energy [11,12], biomass [13,14], ground heat [15] or waste heat [16]. No conventional mode such as 220 V electricity is available for these energies, and the utilization of these energies demands specific design and sensitivity to environmental circumstances. There is a direct correlation between the amount of water needed and the amount of solar radiation received. Furthermore, passive designs can make use of sunrise, sunset and the temperature differential between day and night.

Adsorbent selection is also influenced by the type of energy supplied and the temperature of the heat source, as each adsorbent has a distinct regeneration temperature. This is more apparent when solar energy and waste heat are used, as the heat source's temperature is limited. However, heat pumps [17] and solar concentrators [11,18] can be used to raise the source temperature.

Furthermore, Cattani, Cattani and Magrini [19] proposed a Global Evaluation Index (GEI) to investigate all useful effects of atmospheric water generation. Solar-powered atmospheric water harvesting techniques are studied worldwide and novel approaches are developed on a regular basis. Desiccant materials combined with a solar still and collector or concentrator are a key strategy for increasing solar power and enhancing the efficiency of SPAWH. The system is cost-effective, effortless and easy to install, particularly in distant places.

Solar-Powered Atmospheric Water Harvesting (SPAWH)

Using sorption/desorption technology to generate water from humid air has been the subject of recent studies globally. SPAWH's main advantage over other technologies lies in its capacity to produce water at low relative humidity. SPAWH can produce water widely from hot deserts to tropical areas depending on the adsorbent. Due to the sensible heat of the device's body and the adsorbent remaining consistent, the rate of energy consumption per unit of water generated is lower than other technologies.

Innovative materials and structural designs allow moisture harvesters to speed up the next-generation development of AWH systems [8]. Many studies have been conducted to enhance AWH systems' productivity. For example, Kumar and Yadav [20] investigated the effect of design parameters on the productivity of the solar glass desiccant box type system (SGDBS) (Figure 1a). The study concluded that suitable design parameters are air gap height of 0.22 m, angle inclination of 30° and effective glass thickness of 3 mm. William, Mohamed and Fatouh [21] introduced a trapezoidal prism made of fiberglass and used solar energy to extract water from the ambient air (Figure 1b). The collector was made of a multi-shelved bed to increase the surface area of the bed. The experiment used cloth and sand as host materials that were soaked with $CaCl_2$. With a system efficiency of 29.3% for cloth and 17.76% for sand, the 30% $CaCl_2$ concentration produced 2.32 kg/m^2/day of evaporated water. Harvesting water from air using a novel design of 1.54 m^2 Scheffler reflector,

Srivastava and Yadav [18] experimentally investigated three absorber salts, namely: $CaCl_2$, LiCl and LiBr with a concentration of 37% and sand as a host material. $CaCl_2$, LiCl and LiBr composites produced a maximum of 115 mL/day, 90 mL/day and 73 mL/day in 270 min, 330 min and 270 min, respectively, while the annual cost for the production/L of water amounts to \$0.53, \$0.71 and \$0.86. Talaat et al. [22] investigated the parameters that affect the performance of a finned-type solar-powered portable apparatus, which is used to extract water vapor from atmospheric air through a cloth layer saturated with the solution of $CaCl_2$ (Figure 1c). This apparatus is made of two-faced layers of the conical finned absorber and transparent cover. At night, the conical-absorber soaked moisture, and throughout the day, the absorber was tightly covered with the conical transparent cover and then exposed to the sunlight. The system produced water that ranged from 0.33 kg/m^2/day to 0.63 kg/m^2/day.

Khechekhouche et al. [23] examined the productivity of double glazing solar still and conventional solar still (0.5 × 0.5 m). The results showed that the water yield of double glazing was reduced by 56% in comparison with conventional solar still. A similar approach was conducted by Kumar et al. [24] to compare conventional pyramid-shaped solar still (CPSSS) and air-packed pyramid-shaped solar still (APPSSS) with double glazing (Figure 1d). Due to the air-packed cover, the APPSSS was found to perform less than the CPSSS. Khalifa and Hamood [25] examined the impact of insulation thickness and Elango and Murugavel [26] and Al-Karaghouli and Alnaser [27] conducted experiments to examine the impact of insulation on solar still productivity. PV panel integrated solar still performance was studied by Manokar et al. [28] and Manokar et al. [29]. Sibie, El-Amin and Sun [30] introduced mathematical modeling and simulation to explain the absorption process of three anhydrous salts for water generation in a low humidity climate.

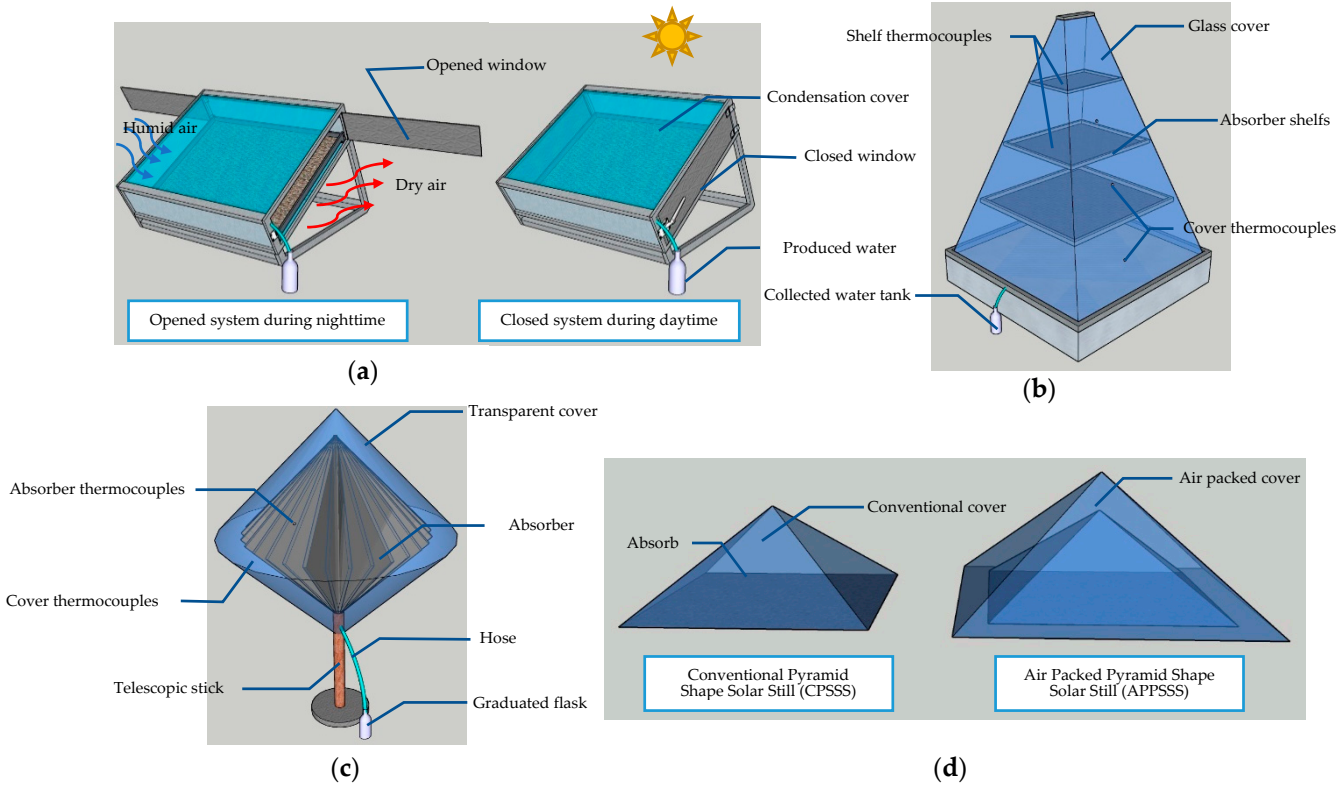

Figure 1. (**a**) Solar glass desiccant box type system (SGDBS), adopted from [20]; (**b**) Trapezoidal prism solar collector, adopted from [21]; (**c**) Double-faced conical finned absorber, adopted from [22] and (**d**) traditional pyramid-shaped solar still and air-filled pyramid-shaped solar still, adopted from [24].

So far, major studies and reviews have been involved in developing adsorbents in terms of the mass of water adsorption and the adsorption/desorption kinetics. The importance of adsorbents cannot be overstated; however, the performance of an AWH system can be affected by a variety of factors. Even if an ideal adsorbent exists, this does not ensure that the system will work properly. Furthermore, condensation surface wettability and vapor droplet contact angle value affect the condensation mechanism, which in turn affects the efficiency of solar stills [31,32]. Similar to other adsorption applications, mass and heat transfer may play an important part in the system's overall performance [33,34]. However, this study only focuses on the heat transfer of different glazing materials.

The main drawback of SPAWH is the low water yield and poor latent heat during the condensation process. Several design modifications were added to boost the SPAWH's water production. The Inclined Solar Still (ISS) is an example of a SPAWH. However, only limited progress was made in the development of ISS. The ISS includes the following benefits added to its design: the flexibility in inclination angle that improved effective area, the direct projection of solar radiation toward the basin and a higher evaporation rate [35]. Further evaporation and condensation mechanisms are vital to enhancing the overall solar still efficiency [36]. Radiation from the sun is the source of energy heat for solar still. Thus, to increase the evaporation rate of absorbers and system efficiency, maximum utilization of solar heat is crucial to gain more water yield. Thus, this study aims to investigate the effect of glazing materials on the thermal performance of SPAWH and its water generation. Table 1 summarizes the main research studies conducted on atmospheric water harvesting (AWH) using the sorption/desorption technique.

Table 1. A survey of studies conducted on atmospheric water harvesting (AWH) systems using desiccants.

Ref	Location	Procedure	Desiccant	Water Production	Efficiency (%)
[37]	Egypt	Experimental and theoretical	$CaCl_2$/sand	1.2 L/m^2/day	-
[38]	Egypt	Experimental	$CaCl_2$/saw wood and cloth	2.5 L/m^2/day	90–95%
[39]	China	Experimental	$CaCl_2$/MCM-41	1.2 kg/m^2/day	-
[40]	Saudi Arabia	Experimental	$CaCl_2$/sand	1.0 L/m^2/day	-
[41]	India	Experimental	Silica gel	200 mL/kg/day	-
[20]	India	Experimental	$CaCl_2$/saw wood	180 mL/kg/day	-
[42]	India	Experimental	$CaCl_2$/vermiculite/saw wood	195 mL/kg/day	-
[21]	Egypt	Experimental	$CaCl_2$/cloth	Cloth = 2320 gm/m^2 Sand = 1235 gm/m^2	Cloth = 29.3% Sand = 17.76%
[43]	China	Experimental	LiCl/consolidated active carbon	14.5 kg/40.8 dry sorbent/day	-
[18]	India	Experimental	LiCl, $CaCl_2$ and LiBr	LiCl = 90 mL/1.54 m^2/day $CaCl_2$ = 115 mL/1.54 m^2/day LiBr = 73 mL/1.54 m^2/day	-
[22]	Egypt	Experimental and theoretical	$CaCl_2$/cloth	0.33–0.63 kg/m^2/day	22.56%
[44]	Egypt	Experimental and mathematical	$CaCl_2$/cloth	1.5 L/m^2/day	17%
[45]	Saudi Arabia	Experimental and theoretical	$CaCl_2$/Cotton cloth	0.51 L/kg (dry sorbent)/day	24.61%

2. Experimental Setup and Measurements

The thermal performance of glazing and water production from atmospheric air were investigated based on two phases, as shown in Figure 2. The first phase is a laboratory test of glass and acrylic properties in terms of solar spectrum transmission and solar power transmission. The second phase covered an experimental study to examine water production and systems efficiency of glass and acrylic glazing systems.

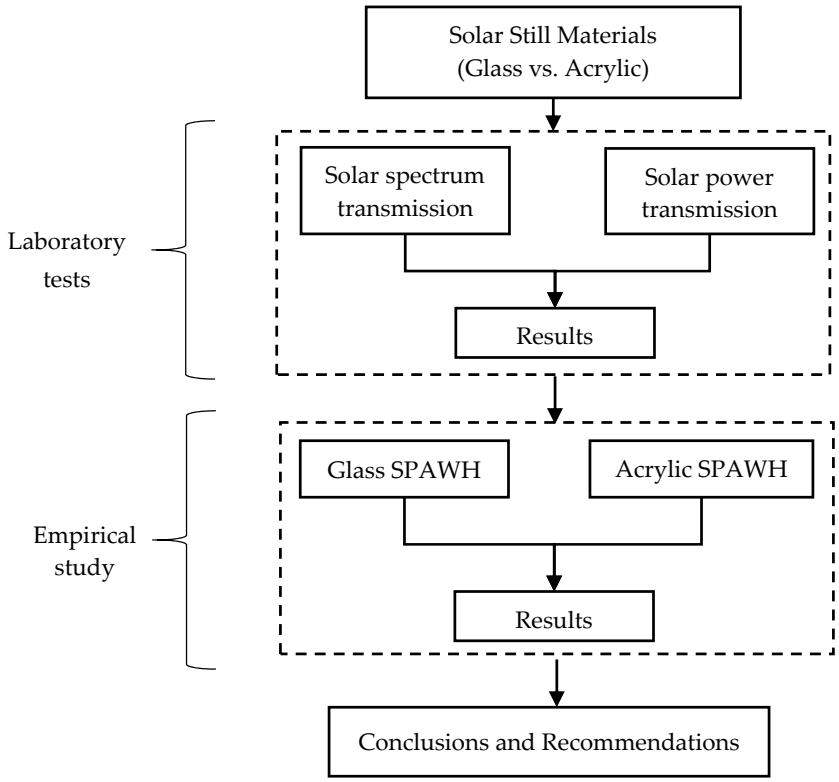

Figure 2. Research process flow.

2.1. Laboratory Tests

Understanding glazing specifications is critical for increasing heat transfer and storage; hence, the efficiency of the atmospheric water harvesting system (SPAWH). In this phase, a comparison between acrylic and glass materials was conducted in terms of their solar spectrum transmission and solar power transmissions (Figure 3). The scientific name of the acrylic used is poly(methyl methacrylate) (PMMA) and classified as a transparent thermoplastic.

(**a**) (**b**)

Figure 3. (**a**) EDTM-SS2450 instrument to measure the solar spectrum; (**b**) EDTM-SP2065 instrument to measure transmission power.

Five samples of each glass and acrylic Perspex (20 cm × 20 cm) with thicknesses: 3, 4, 5, 6 and 8 mm were tested. Solar spectrum transmission was measured using the EDTM-SS2450. Generally, solar radiation contains three primary forms of light: ultraviolet (UV), visible and infrared (IR).

In addition, EDTM-SS2450 measures the Damage Weight Transmission (Tdw) of solar radiation. Solar radiation contributes to the damage of materials through fading and the

general breakdown of the fabric structure. For example, an 80% Tdw will cause more fading than a 20% Tdw. This evaluation will assist in considering the effect of the glazing type on the materials inside SPAWH in long-term usage. Additionally, EDTM-SP2065 instrument was used to measure the power and solar transmission of glass and acrylic samples (Figure 3).

Table 2 shows the comparison between glass and acrylic samples' properties in terms of the solar spectrum and power transmission. For ultraviolet energy UV (315–380 nm), the results showed that UV transmission for glass was almost similar for all samples with a range of 57–59% for glass thickness of 8 mm to 3 mm. In contrast, for acrylic samples, UV energy presented a wide variation with a maximum level of 74% for the acrylic thickness of 3 mm and 5% for 8 mm of acrylic thickness. Turning into visible light (380–780 nm), acrylic samples recorded higher transmission values than glass samples. Visible light transmission gradually increased from 91–95% for acrylic samples and 89–90% for glass samples of 3 mm–8 mm. For the near-infrared radiation IR (780–1700 nm), increasing glass thickness reduced the amount of transmission with a range from 80–70% for a glass thickness from 3–8 mm. In contrast, an increase in acrylic thickness slightly increased the amount of IR transmission from 90–92% for acrylic thickness from 3–8 mm. As infrared radiation IR energy typically refers to long waves, which are mainly responsible for heat radiation transfer, acrylic glazing might experience high heat loss compared to glass. However, the damage weight for glass was less than acrylic for a thickness of 3 mm (glass 84% and acrylic 88%). Damage weight of glass increased from 84–86% with the rise in samples' thicknesses from 3–8 mm but reduced from 88–77% for the same thicknesses of acrylic samples. Total power transmission percentages were similar for all acrylic samples with 91%. However, glass power transmission ranged from 82–70% for samples' thicknesses from 3–8 mm, as shown in Table 2. Therefore, the amount of heat that escapes from glass is less than acrylic, which might increase SPAWH heat and system efficiency.

Table 2. Comparison between glass and acrylic samples' properties.

Properties of Glass (G) vs. Acrylic (A)										
	EDTM-SS2450								EDTM-SP2065	
Thickness>	UV (315–380 nm) %		Visible (380–780 nm) %		IR (780–1700 nm) %		Damage Weight %		Transmission Power %	
Glazing	G	A	G	A	G	A	G	A	G	A
3 mm	59	74	89	91	80	90	84	88	82	91
4 mm	59	17	89	92	77	91	85	78	78	91
5 mm	59	15	89	93	73	91	85	78	74	91
6 mm	59	7	90	94	73	92	86	76	72	91
8 mm	57	5	90	95	70	92	86	77	70	91

2.2. Experimental Study

The study conducted field experiments at the faculty of the built environment, the University of Malaya in Kuala Lumpur, Malaysia. The study targeted two periods of dry and wet seasons, around February and August (Figure 4). Two atmospheric water harvesting systems (SPAWH) were compared in terms of thermal performance, water quantity and system efficiency using glass and acrylic materials as glazing. More details about these two systems are explained in the following sections.

In this experimental study, the solar-powered atmospheric water harvesting systems (SPAWH) were designed, manufactured and used, as shown in Figure 5. The first SPAWH is fabricated by assembling a clear Perspex acrylic box (60 cm (L) × 60 cm (W) × 30 cm (H)). The upper cover is adjusted to be removable for the processes of sorption and desorption.

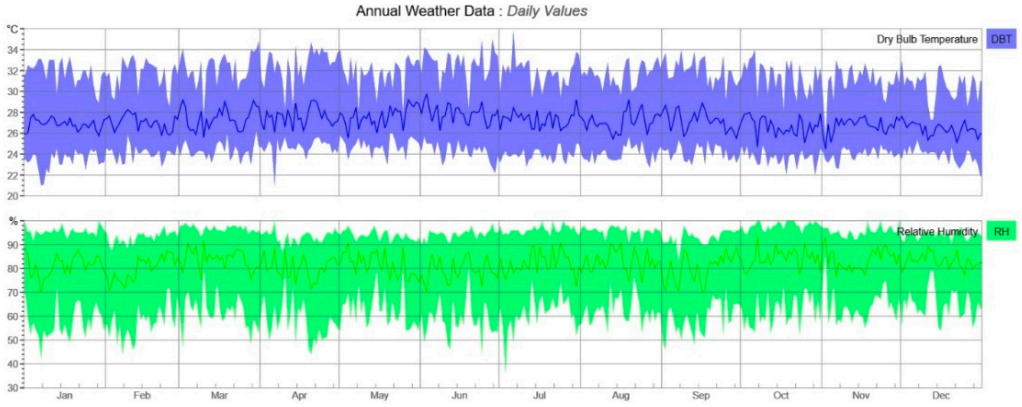

Figure 4. Weather data of air temperature and relative humidity for Kuala Lumpur, Malaysia [46].

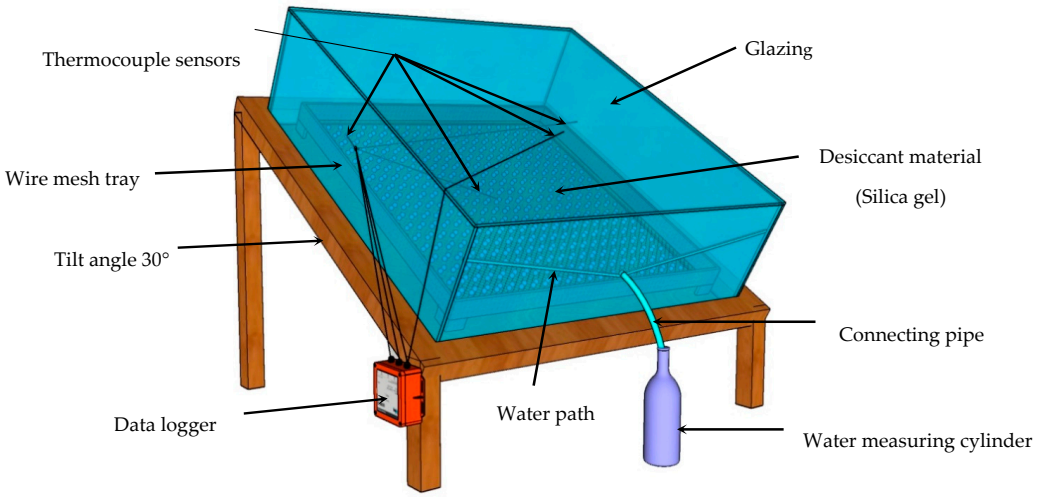

Figure 5. Graphical diagram of the SPAWH.

For collecting condensed water, a pipe was connected to the system. During the regeneration process, a transparent 3 mm acrylic, which acts as a condenser, is used for glazing. The desiccant material (silica gel) was held by a wire mesh sized 3 mm × 3 mm, screwed to the L shape frame (Figure 6). A measuring cylinder with a reading of 5 mL is used to measure the quantity of water generated. Figure 7 displays the desiccant material before and after the absorption process in the SPAWH. Table 3 provides more details about SPAWH main parts.

Table 3. Main parts of SPAWH.

SPAWH Parts	Description
Main container	Two containers of glass and acrylic were used due to their sufficient strength and long life. The size of each SPAWH is 0.6 m × 0.6 m × 0.3 m. The top cover was modified so that it can be removed for the nighttime absorption process. A water pipe with a slight slope was fitted on the front side to collect droplets from the glass/acrylic after condensation.
Glazing	The first container used a glass of 3 mm thickness for glazing, while the second container used a clear Perspex acrylic of 3 mm as glazing. This glazing also acted as a condenser during the process of regeneration. The sunlight of shorter wavelengths can enter the SPAWH by the glass and clear acrylic and captured radiation of longer wavelength after heating the desiccant material. The greenhouse effect was generated within the SPAWH.

Table 3. *Cont.*

SPAWH Parts	Description
Wire mesh tray	Inside SPAWH, the desiccant material was stored on the wire mesh of steel wire. The wire mesh is 3 mm × 3 mm in dimensions. The aluminum L shape frame was fastened with a wire mesh.
Connecting pipe	Between the container and the measuring cylinder, the connection pipe was attached. This pipe provided a path to flow water droplets.
Water measuring cylinder	A water measuring cylinder for water collection was used outside the SPAWH. The water was collected directly through the connecting tube to the measuring cylinder. There were measuring marks on the bottle that indicate the amount of water collected. The minimum quantity of water measurable was 5 mL.
Desiccant material	For atmospheric water extraction, silica gel was used as a desiccant material. To this end, for each SPAWH, 2 kg of silica gel was used. In regenerated form, the color of silica gel was blue, whereas it turned to a rose color in a saturation state. This color transformation is due to cobalt chloride (Figures 6 and 7).

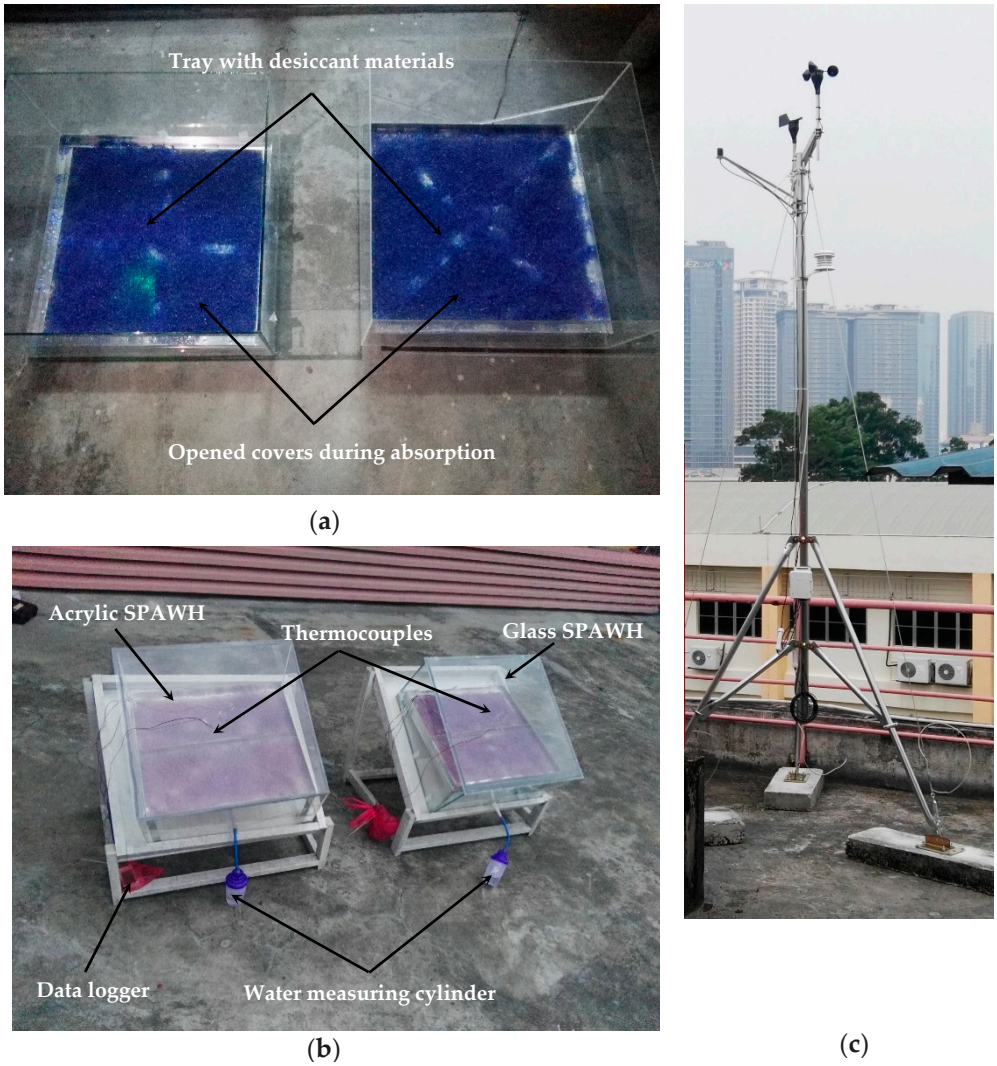

Figure 6. Experimental setup photograph: (**a**) absorption process during the night; (**b**) regeneration process during day and (**c**) Mini meteorological station.

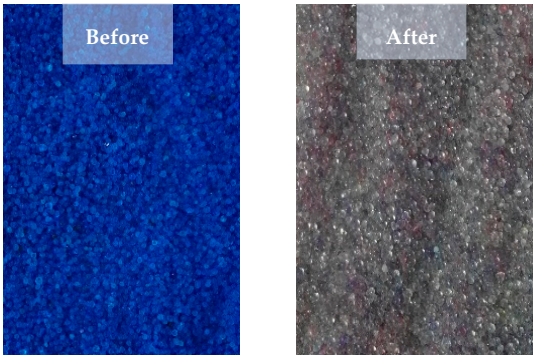

Figure 7. Desiccant material before and after absorption process.

2.2.1. Measuring Instruments and Sensor Specifications

During laboratory tests and empirical experiments, various parameters were measured, as shown in Table 4. All laboratory and experimental data were recorded in the study field.

2.2.2. Experimental Procedure

Two main stages were performed to investigate the atmospheric water production using the desiccant materials (Figure 8):

(a) Adsorption process at night. In this step, water vapor is taken up by the adsorbent in contact with ambient air.
(b) Desorption and condensation process on the next day. The desiccant is isolated from the ambient air and the solar heat is applied to desorb the water vapor, which is finally condensed and collected.

The desiccant material was exposed to the atmosphere from 7:00 p.m. in the evening to 7:00 a.m. As a result of the difference in vapor pressure between the desiccant material surface and air, moisture from the ambient air is adsorbed by the desiccant material. The adsorption rate decreases as time goes by. In the interval of 30 min, the adsorption rate was measured using a weighing machine. The cover was closed in the morning at 7:00 a.m. and the SPAWH was tightly sealed for sunlight exposure in the regeneration process. The difference in vapor pressure between the desiccant surface and the air in the inner space of the box increases as the temperature of the desiccant material increases. The absorbed moisture is then transferred to the inner air and raises the vapor pressure. As the solar intensity increases, mass vapor flows from the desiccant substance to the indoor air until it reaches the saturation point. The water vapor then begins to condense on the inside of the glass cover, forming tiny drops. These tiny drops slip across the glass surface and land in the water collection tray. Finally, the collected water flows through a connecting pipe to the water measurement cylinder due to the slope in the water collection tray. The volume of water collected was measured manually at an interval of 30 min. In addition, the system temperature and meteorological data were recorded during the regeneration process.

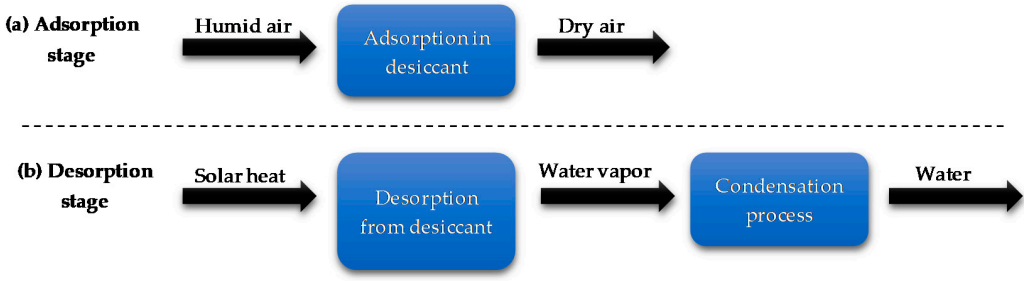

Figure 8. Adsorption/desorption stages of SPAWH.

Table 4. Specifications of measuring instruments and sensors.

	Instruments/ Sensors	Models	Accuracy	Ranges	Characteristics
Lab tests	Solar spectrum transmission	EDTM-SS2450	±3%	315 nm–1700 nm	Accurate solar spectrum transmission and damage weight. Application: Measuring glass and acrylic samples (3, 4, 5, 6 and 8 mm).
	Solar power meter	EDTM-SP2065	N/A	N/A	Measures the power of incident solar radiation per unit area entering the sensing zone of the meter. Application: measuring glass and acrylic samples (3, 4, 5, 6 and 8 mm).
Experimental sensors	Weather station data logger	H21-USB	-	-	A weatherproof data logger for multi-channel monitoring of microclimates. It includes five smart sensor inputs.
	4-Channel Thermocouple Data Logger	UX120-014M	±0.21 °C	−260 °C to 1820 °C	To measure the surface temperature of the desiccant material, the inner and outer side of the glass/acrylic top cover and the inner side of the SPAWH.
	Thermocouple probes	Type J 6 ft Beaded	±2.2 °C	0 °C to 250 °C	It contains 1.8 m (6′) of isolated 30-AWG cable wound for a built-in spool caddy/subminiature connector. Application: stick on the glazing surface and connect with the thermocouple data logger.
	Outdoor relative humidity	S-THB-M002	±0.1% RH	0–100%	Highly precise measurement of relative humidity. Long-term humidity stability.
	Outdoor air temperature	S-THB-M002	±0.21 °C	−40 °C to 75 °C	Accurate measurement of ambient air temperature.
	Solar radiation intensity	S-LIB-M003	±10 W/m^2 (±5%)	0 to 1280 W/m^2	To measure light intensity. This sensor has a measurement range of 0 to 1280 W/m^2 over wavelengths from 300 to 1100 nm.
	Solar radiation shield	RS3-B	-	-	To improve the precision of temperature measurements, use the RS3-B Solar Radiation Shield with HOBO external sensors in places exposed to sunlight.
	Electronic balance	AJ-12KE	±0.1 g	0 g–12,000 g	Quick response and stable indication balance. Applications: (1) To measure the desiccant material before experiments. (2) To measure the absorption rate during nighttime. (3) To measure the desiccant material after the regeneration process.

The adsorption and regeneration rates were determined based on weight. The rate of adsorption and regeneration was calculated using the following formula [47]:

$$G_a = m_{wS}\frac{dw}{dt} \quad (1)$$

where G_a refers to the adsorption rate (kg/h), m_{wS} is the adsorber's weight (wet basis) in kg, dw/dt is moisture content in the desiccant material throughout the time interval.

$$G_r = m_{dS}\frac{dw}{dt} \quad (2)$$

where G_r is the regeneration rate (kg/h) and m_{dS} is the adsorber's weight (dry basis) in kg.

3. Results and Discussion

The main objective of this study is to compare the performance of SPAWH design using different glazing materials in the tropics. For this purpose, the two glazing systems were analyzed in terms of the adsorption rate of desiccant materials, the temperature of SPAWH at several points, water production from each system and cost analysis.

3.1. Adsorption Rate of Desiccant Materials

Both SPAWH systems (glass and acrylic) covers were opened during nighttime to measure the adsorption rate of the desiccant materials. The adsorption rate was manually recorded for 12 h from 7:00 p.m. to 7:00 a.m. with half-hour intervals. Generally, both systems' adsorption rate was similar, as the same weight of desiccant materials was placed in each system (2000 g of silica gel). Figure 9 shows the adsorption rate alongside relative humidity and ambient air temperature. At the initial stage, maximum adsorption rate was recorded at 0.080 kg/h and 0.082 kg/h followed by 0.044 kg/h and 0.052 kg/h on 21 February 2020 and 31 July 2020, respectively.

The behavior of adsorption rate returns to the characteristic of pores in the desiccant materials. Initially, all pores in silica gel were empty and with the progression of time, most pores started to be filled. Subsequently, the adsorption rate decreases with time. However, the adsorption rate on 31 July 2020 was a bit higher than on 21 February 2020, as shown in Figure 9. The relative humidity of outdoor air on 31 July 2020 was higher compared to 21 February 2020. In addition, the adsorption rate efficiency of silica gel reduces with an ambient temperature of more than 25 °C [48], which is slightly lower than the adsorption rate on 21 February 2020.

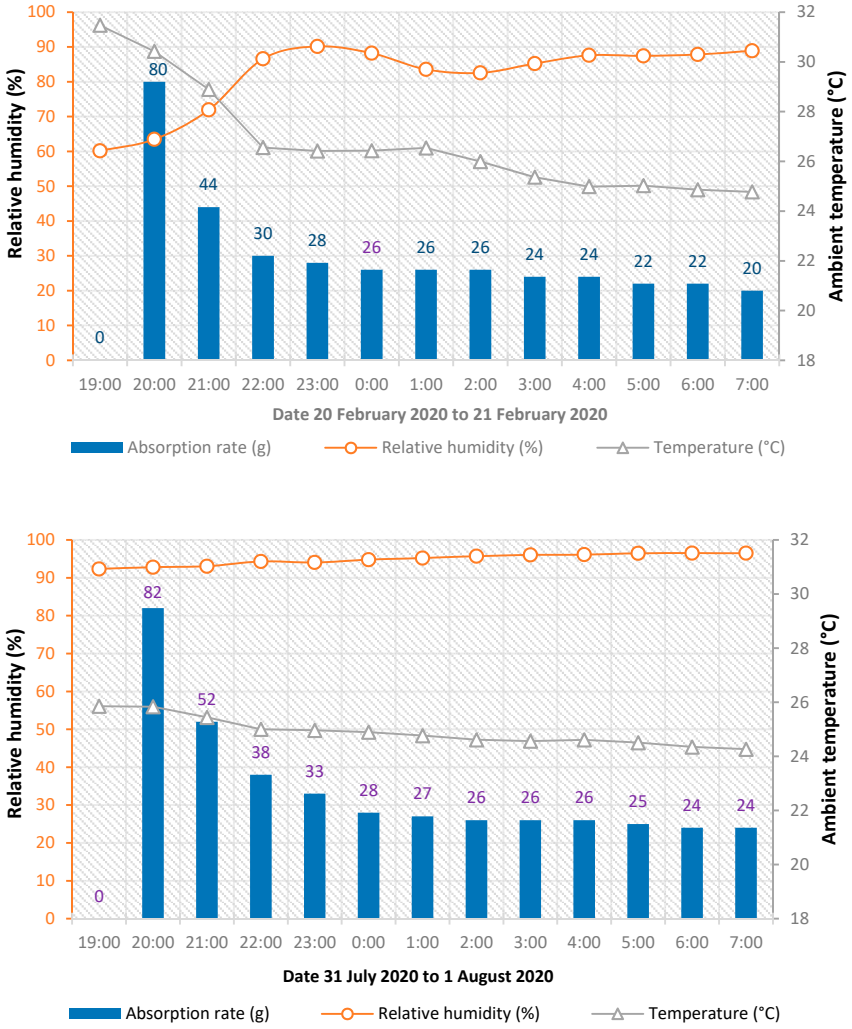

Figure 9. Adsorption rate, ambient air temperature and relative humidity.

3.2. Temperature Variation in the Systems

The water production and system efficiency are mainly affected by temperature variation in SPAWH. Four thermocouple probes were attached on desiccant materials, inner

side, inner glazing cover and outer glazing cover of each SPAWH to examine temperature behavior in the systems. As the Solar-Powered Atmospheric Water Harvesting with acrylic glazing (SPAWHa) properties allow more solar energy to enter into the desiccant materials (see Table 2), the temperature increased more than the Solar-Powered Atmospheric Water Harvesting with glass glazing (SPAWHg) at the initial period between 9:00 a.m. and 10:30 a.m. In contrast, the thermal conductivity of glass is higher than in acrylic. After 10:30 a.m., the temperature in the SPAWHg was higher. As the power transmission percentage of the glass is lower than acrylic (see Table 2), the heat loss rate in SPAWHg was less than SPAWHa. Subsequently, the net heat in SPAWHg was higher than SPAWHa, which led to higher performance of the SPAWHg. However, the penetration of the solar irradiance was also reduced by water droplets on the condensation surface.

Figures 10 and 11 show the variation in desiccant temperature and solar radiation with time in both SPAWH (glass and acrylic). In SPAWHg, the maximum desiccant temperature reached 79 °C and 73 °C, whereas for SPAWHa reached 77 °C and 65 °C on 21 February 2020 and 1 August 2020, respectively. Generally, the desiccant temperature in SPAWHg was higher than SPAWHa during the daytime.

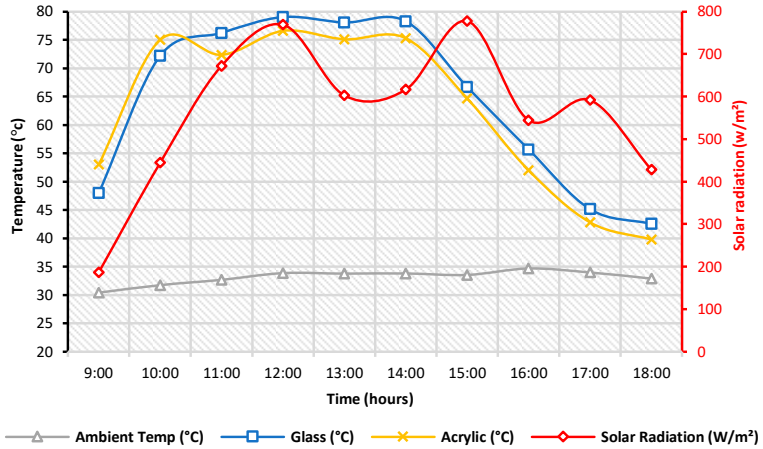

Figure 10. Variation in solar intensity and temperature of desiccant materials on 21 February 2020.

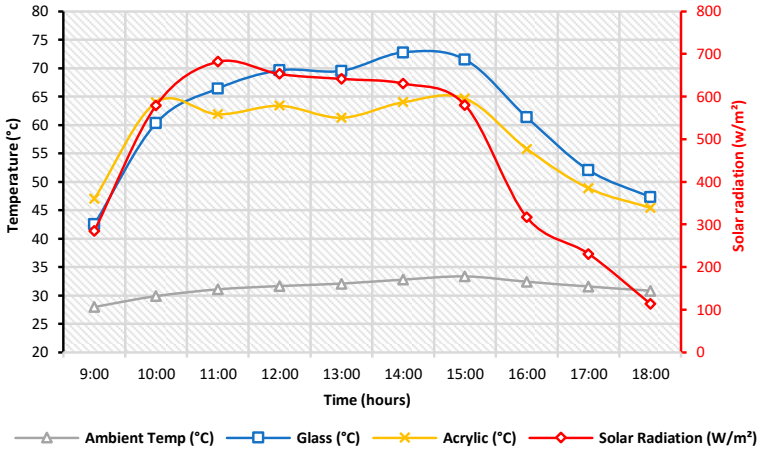

Figure 11. Variation in solar intensity and temperature of desiccant materials on 1 August 2020.

Figure 12 shows the internal side temperature of SPAWH and solar intensity with time on 21 February 2020 and 1 August 2020. The internal side of SPAWHg has a higher temperature compared to SPAWHa. In SPAWHg, the maximum temperature reached 56 °C and 50 °C, whereas SPAWHa reached 54 °C and 48 °C on 21 February 2020 and 1 August 2020, respectively. In the same way, for SPAWHg, the temperature on the inner cover and outer cover was higher than SPAWHa, as shown in Figures 13 and 14. However,

the surface temperature in the SPAWHg for the inner and outer cover side was higher than SPAWHa at about 3–6 °C. This can be attributed to the higher latent temperature of the glass. The maximum surface temperature of the inner SPAWHg cover was 59 °C and 53 °C, whereas SPAWHa was 54 °C and 50 °C on 21 February 2020 and 1 August 2020, respectively. In comparison, the outer side cover was 54 °C and 49 °C for SPAWHg and 51 °C and 46 °C for SPAWHa on 21 February 2020 and 1 August 2020, respectively.

When energy is transmitted into an adsorbent bed, some of this energy was used to raise the temperature, which is known as sensible heat [49]. During the transition to the adsorption phase, this heat was most frequently released back into the atmosphere. All adsorption systems lose energy efficiency due to sensible heat, which cannot be avoided. The lower the ratio of sensible heat to adsorption heat, the more efficient the device will be at capturing energy. Due to this, the desorption enthalpy should be given greater consideration [50]. A reduction in adsorption enthalpy can boost daily production capacity due to the limited availability of energy resources.

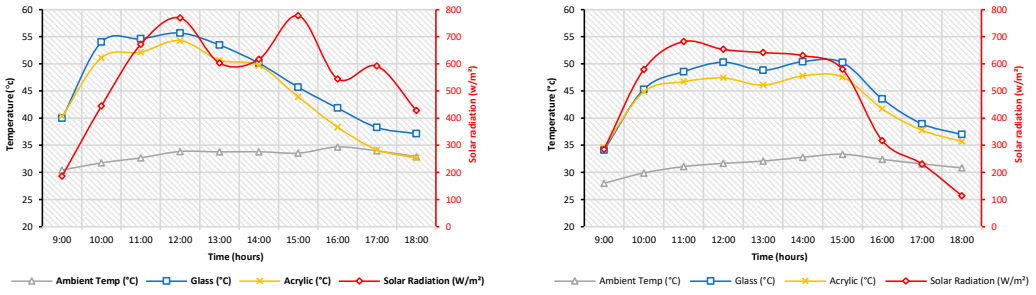

(**a**) (**b**)

Figure 12. Variation in solar intensity and internal side temperature: (**a**) 21 February 2020 and (**b**) 1 August 2020.

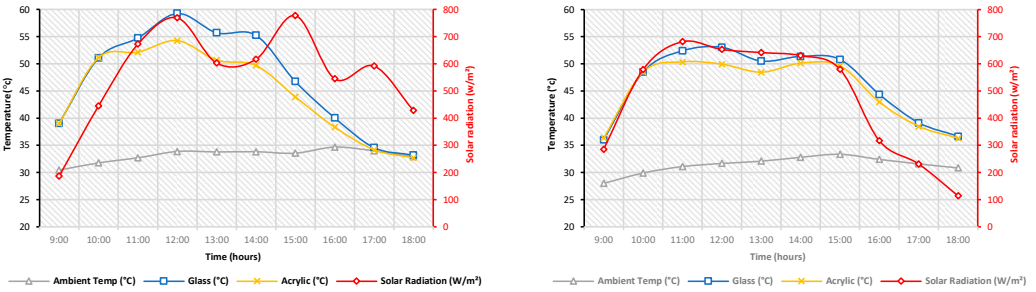

(**a**) (**b**)

Figure 13. Variation in solar intensity and inner cover temperature: (**a**) 21 February 2020 and (**b**) 1 August 2020.

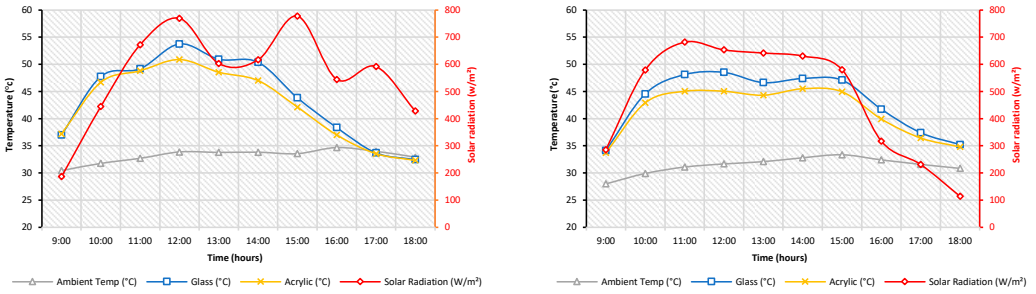

(**a**) (**b**)

Figure 14. Variation in solar intensity and outer cover temperature: (**a**) 21 February 2020 and (**b**) 1 August 2020.

3.3. Variation in Water Production

The water production rate of SPAWH depends on several variables that affect the system efficiency, such as solar intensity, ambient air temperature, relative humidity during the night, desiccant adsorption capacity and temperature needed to release water (generation process). However, there are other variables that affect water production, such as proper design and tightness of SPAWH and glazing materials and properties in terms of the solar spectrum and power transmissions. Although this study used the same desiccant material (silica gel) with the same weather circumstances and identical SPAWH design and dimensions (L60 cm × W60 cm × H30 cm), the difference is only in the glazing system.

The water production and system efficiency in SPAWHg were higher than SPAWHa. As shown in Figures 15 and 16, water production from SPAWHg was 220 and 180 g/day, whereas for SPAWHa, it was 160 and 125 g/day on 21 February 2020 and 1 August 2020, respectively. Although acrylic allowed more solar energy transmission into the SPAWH, the thermal conductivity of the glass is higher, which led to rising the net heat of SPAWHg. In addition, the characteristics of glass reduce heat loss from SPAWHg into the surroundings, which leads to an increase in the temperature inside SPAWHg and generates more water. The rate of energy entry and temperature of the condenser has an effect on desorption kinetics as well [51]. Both factors are no longer constant if solar energy is used. As a result of the overall heat increment, the overall performance of SPAWH improved when the design of the adsorption-desorption system was efficient.

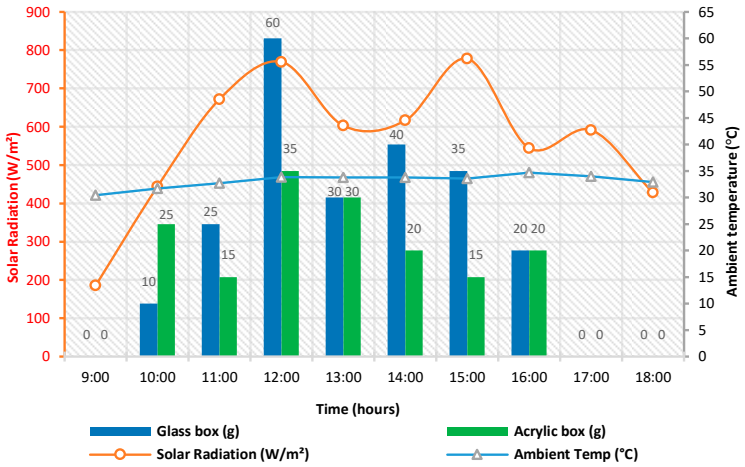

(**a**)

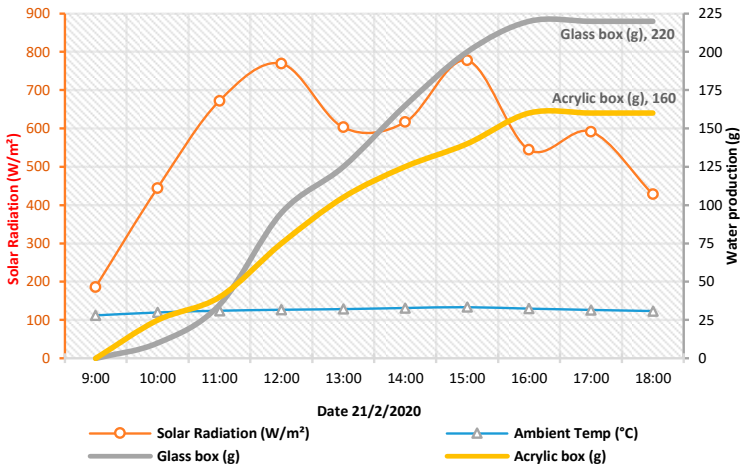

(**b**)

Figure 15. Variation of water production by glass and acrylic glazing systems on 21 February 2020: (**a**) hourly water produced and (**b**) accumulated water produced.

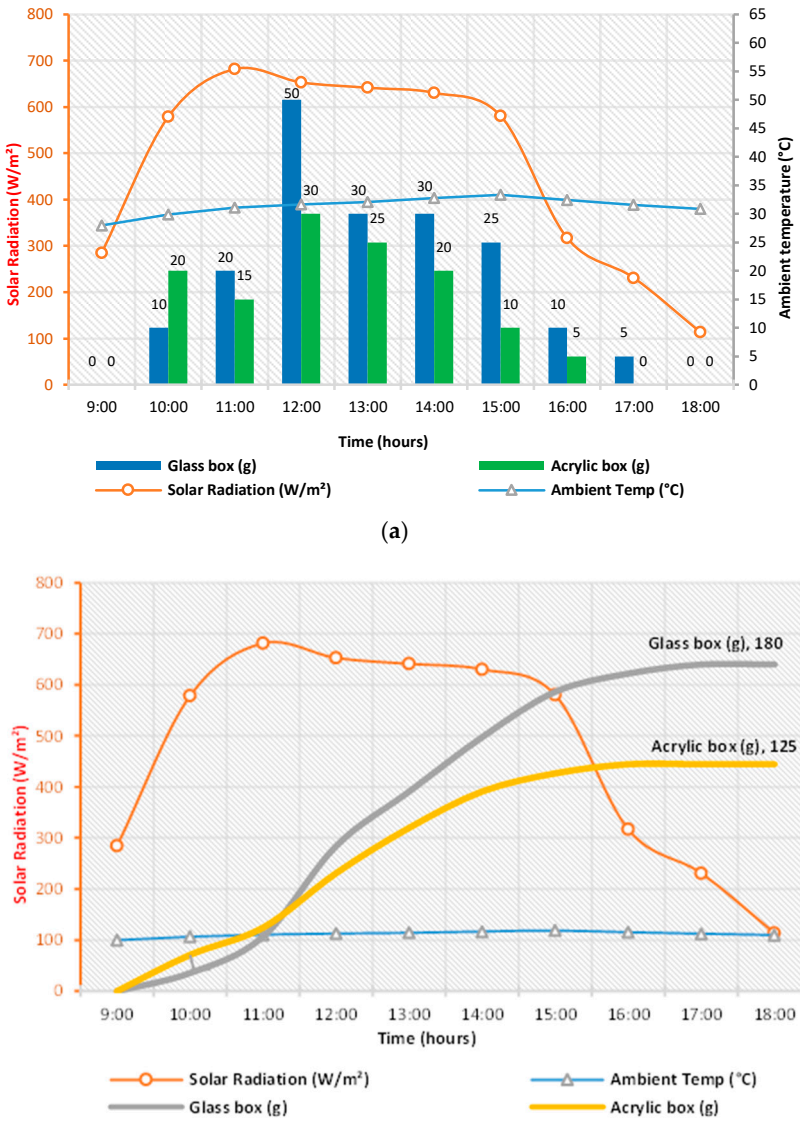

Figure 16. Variation of water production by glass and acrylic glazing systems on 1 August 2020: (**a**) hourly water produced and (**b**) accumulated water produced.

3.4. Cost Analysis of the SPAWH

In order to determine the costs of water production for the unit, a cost analysis is conducted. The unit works every day of the year. The principal cost analysis estimation parameters are [22,52]:

The capital recovery factor, *CRF*, which is estimated by the following relationship,

$$CRF = \frac{I(I+1)^N}{(I+1)^{N-1}} \quad (3)$$

where I is the annual interest rate, which is assumed to be 12% and N is the number of life years, which is assumed to be 10 years for glass and 5 years for acrylic. The fixed annual cost, *FAC*, can be calculated by multiplying the unit's present capital cost (*PC*), as shown in Table 5 (which is \$75.15 (USD) for glass SPAWH and \$81.15 (USD) for acrylic SPAWH) and *CRF* as,

$$FAC = PC \times CRF \quad (4)$$

Table 5. Cost breakdown of AWH systems.

Parameter	Cost of Glass AWH System (USD)	Cost of Acrylic AWH System (USD)
Glazing	22	28
Wire mesh tray	5	5
Desiccant materials (2 kg)	14	14
Wood table	15	15
Paint	2.5	2.5
Water collecting cylinder	1.25	1.25
Connecting pipe	0.4	0.4
Production	15	15
Total cost	75.15	81.15

The sinking fund factor, *SFF*, can be calculated as,

$$SFF = \frac{I}{(I+1)^{N-1}} \quad (5)$$

The annual salvage value, *ASV*, is determined by multiplying *SFF* by the salvage value, *S*, which is calculated as,

$$S = 0.2 \times PC \quad (6)$$

$$ASV = SSF \times S \quad (7)$$

The unit's annual maintenance operational cost, *AMC*, can be calculated as,

$$AMC = 0.15 \times FAC \quad (8)$$

The annual cost is estimated as,

$$AC = FAC + AMC - ASV \quad (9)$$

To calculate the cost produced kilogram of water generated (*CPK*), the annual cost can be divided by total produced water over the year, *M*, as,

$$CPK = \frac{AC}{M}\ (10) \quad (10)$$

The cost of a kilogram of produced water is determined by this cost analysis with \$0.18 USD/kg and \$0.40 USD/kg for glass and acrylic SPAWH, respectively.

4. Conclusions

Two solar-powered atmospheric water harvesting systems (SPAWH) were designed and manufactured with different glazing materials: glass and acrylic in the tropics. This desiccant adsorbs moisture from humid air and then regenerates it with solar heat. The system operation and experimental results were thoroughly discussed and the main findings can be summarized as follows:

- Although acrylic glazing allows more solar transmission compared to glass, a system with acrylic has a low thermal conductivity compared to glass. The data showed that the desiccant material's temperature of the SPAWHa was higher than SPAWHg at the first two hours of the experimental period; however, the desiccant materials of the SPAWHg recorded higher temperature along with the daytime.

- The power transmission in glass samples (3 mm–8 mm) is reduced from 82–70%, while, for acrylic samples, the percentage was maintained for all samples with different thicknesses and achieved 91%. These findings showed that the SPAWHg desiccant materials maintained higher temperatures along with the daytime with less heat loss, hence, increased system efficiency.
- Water production from SPAWHg was 220 g/day on 21 February 2020 and 180 g/day on 1 August 2020. SPAWHa was 160 g/day on 21 February 2020 and 125 g/day on 1 August 2020. These results showed that during a dry season, when ambient air temperature and solar radiation are high, the system could generate 22% water in SPAWHg and 28% in SPAWHa more than in a wet season because the relative humidity is high and ambient air temperature is low.
- The maximum water produced by SPAWHg and SPAWHa was 0.61 L/m^2/day and 0.44 L/m^2/day, respectively. That imputes to glass properties that enjoy higher thermal conductivity and mitigate heat loss, hence, increasing the system efficiency.
- The cost analysis shows that the kilogram of produced water costs 0.18 USD/kg and 0.40 USD/kg for glass and acrylic SPAWH, respectively.
- Atmospheric water can be produced using SPAWH in the tropical climate, which enjoys a high percentage of moisture content.

For enhancing AWH systems' productivity, this study investigated two different glazing materials, namely, glass and acrylic in terms of their thermal performance. However, testing other transparent materials (e.g., plastic, Polyvinyl chloride (PVC), etc.) with novel designs to raise thermal performance and increase the productivity of SPAWH is needed. In addition, this study compared the systems in February and August; moreover, the need for long-term testing throughout the entire year might be beneficial. All experiments have been done in one location in Kuala Lumpur; therefore, conducting other experiments in different tropical locations would enhance the system's reliability. Future research is needed to investigate the efficiency of SPAWH systems in the tropics using different designs and shapes with different desiccant materials. Moreover, examining the condensation surfaces' wettability and vapor droplet contact angle value of novel coated glazing materials would enhance the efficiency of SPAWH systems. However, considering economic, environmental and social aspects are crucial for the reliability and productivity of SPAWH systems.

Author Contributions: Conceptualization, H.S.A.-D., M.A.I. and K.M.A.-O.; methodology, H.S.A.-D., M.A.I. and K.M.A.-O.; validation, H.S.A.-D. and M.A.I.; formal analysis, H.S.A.-D.; investigation, H.S.A.-D. and M.A.I.; resources, H.S.A.-D. and M.A.I.; writing—original draft preparation, H.S.A.-D. and M.A.I.; writing—review and editing, H.S.A.-D., M.A.I., Z.A.M.A. and K.M.A.-O.; visualization, H.S.A.-D.; supervision, M.A.I., Z.A.M.A. and K.M.A.-O.; project administration, M.A.I. and Z.A.M.A. All authors have read and agreed to the published version of the manuscript.

Funding: This research received no external funding.

Conflicts of Interest: The authors declare no conflict of interest.

References

1. United Nations. *Revision of World Population Prospects*; UN: New York, NY, USA, 2019.
2. Zhang, S.; Huang, J.; Chen, Z.; Lai, Y. Bioinspired special wettability surfaces: From fundamental research to water harvesting applications. *Small* **2017**, *13*, 1602992. [CrossRef] [PubMed]
3. Shiklomanov, I.A. World freshwater resources. Water in crisis: A guide to the world's freshwaterresources. *Clim. Chang.* **1993**, *45*, 379–382.
4. Eslami, M.; Tajeddini, F.; Etaati, N. Thermal analysis and optimization of a system for water harvesting from humid air using thermoelectric coolers. *Energy Convers. Manag.* **2018**, *174*, 417–429. [CrossRef]
5. Claire, S. *The Last Drop*; Summer Issue; Mazaya: Kabupaten Tasikmalaya, Indonesia, 2002; pp. 22–25.
6. Lorenzo, T.E.; Kinzig, A.P. Double exposures: Future water security across urban Southeast Asia. *Water* **2019**, *12*, 116. [CrossRef]
7. Al-Duais, H.S.; Ismail, M.A.; Awad, Z.A.; Al-Obaidi, K.M. Methods of harvesting water from air for sustainable buildings in hot and tropical climates. *Malays. Constr. Res. J.* **2022**, *15*, 150–168.
8. Zhou, X.; Lu, H.; Zhao, F.; Yu, G. Atmospheric water harvesting: A review of material and structural designs. *ACS Mater. Lett.* **2020**, *2*, 671–684. [CrossRef]

9. Beysens, D.; Milimouk, I. The case for alternative freshwatersources. [Pour les resources alternatives en eau]. *Secheresse* **2000**, *11*, 1–6.
10. Bergmair, D.; Metz, S.J.; de Lange, H.C.; van Steenhoven, A.A. System analysis of membrane facilitated water generation from air humidity. *Desalination* **2014**, *339*, 26–33. [CrossRef]
11. Wang, J.Y.; Liu, J.Y.; Wang, R.Z.; Wang, L.W. Experimental investigation on two solar-driven sorption based devices to extract freshwaterfrom atmosphere. *Appl. Therm. Eng.* **2017**, *127*, 1608–1616. [CrossRef]
12. Wang, M.; Sun, T.; Wan, D.; Dai, M.; Ling, S.; Wang, J.; Liu, Y.; Fang, Y.; Xu, S.; Yeo, J.; et al. Solar-powered nanostructured biopolymer hygroscopic aerogels for atmospheric water harvesting. *Nano Energy* **2021**, *80*, 105569. [CrossRef]
13. Chaitanya, B.; Bahadur, V.; Thakur, A.D.; Raj, R. Biomass-gasification-based atmospheric water harvesting in India. *Energy* **2018**, *165*, 610–621. [CrossRef]
14. Wikramanayake, E.D.; Ozkan, O.; Bahadur, V. Landfill gas-powered atmospheric water harvesting for oilfield operations in the United States. *Energy* **2017**, *138*, 647–658. [CrossRef]
15. Heidarinejad, G.; Rayegan, S.; Pasdarshahri, H. Dynamic simulation of a solar desiccant cooling system combined with a ground source heat exchanger in humid climates. *J. Build. Eng.* **2020**, *28*, 101048. [CrossRef]
16. Ng, K.C.; Thu, K.; Saha, B.B.; Chakraborty, A. Study on a waste heat-driven adsorption cooling cum desalination cycle. *Int. J. Refrig.* **2012**, *35*, 685–693. [CrossRef]
17. Tan, B.; Luo, Y.; Liang, X.; Wang, S.; Gao, X.; Zhang, Z.; Fang, Y. Composite salt in MIL-101 (Cr) with high water uptake and fast adsorption kinetics for adsorption heat pumps. *Microporous Mesoporous Mater.* **2019**, *286*, 141–148. [CrossRef]
18. Srivastava, S.; Yadav, A. Water generation from atmospheric air by using composite desiccant material through fixed focus concentrating solar thermal power. *Sol. Energy* **2018**, *169*, 302–315. [CrossRef]
19. Cattani, L.; Cattani, P.; Magrini, A. Air to water generator integrated systems: The proposal of a global evaluation index—GEI formulation and application examples. *Energies* **2021**, *14*, 8528. [CrossRef]
20. Kumar, M.; Yadav, A. Experimental investigation of solar powered water production from atmospheric air by using composite desiccant material "CaCl2/saw wood". *Desalination* **2015**, *367*, 216–222. [CrossRef]
21. William, G.E.; Mohamed, M.H.; Fatouh, M. Desiccant system for water production from humid air using solar energy. *Energy* **2015**, *90*, 1707–1720. [CrossRef]
22. Talaat, M.A.; Awad, M.M.; Zeidan, E.B.; Hamed, A.M. Solar-powered portable apparatus for extracting water from air using desiccant solution. *Renew. Energy* **2018**, *119*, 662–674. [CrossRef]
23. Khechekhouche, A.; Benhaoua, B.; Manokar, A.M.; Kabeel, A.E.; Sathyamurthy, R. Exploitation of an insulated air chamber as a glazed cover of a conventional solar still. *Heat Transf. Asian Res.* **2019**, *48*, 1563–1574. [CrossRef]
24. Kumar, S.A.; Mohan Kumar, P.S.; Sathyamurthy, R.; Manokar, A.M. Experimental investigation on pyramid solar still with single and double collector cover—comparative study. *Heat Transf. Asian Res.* **2020**, *49*, 103–119. [CrossRef]
25. Khalifa, A.J.; Hamood, A.M. Effect of insulation thickness on the productivity of basin type solar stills: An experimental verification under local climate. *Energy Convers. Manag.* **2009**, *50*, 2457–2461. [CrossRef]
26. Elango, T.; Murugavel, K.K. The effect of the water depth on the productivity for single and double basin double slope glass solar stills. *Desalination* **2015**, *359*, 82–91. [CrossRef]
27. Al-Karaghouli, A.A.; Alnaser, W.E. Experimental comparative study of the performances of single and double basin solar-stills. *Appl. Energy* **2004**, *77*, 317–325. [CrossRef]
28. Manokar, A.M.; Winston, D.P.; Kabeel, A.E.; Sathyamurthy, R. Sustainable freshwaterand power production by integrating PV panel in inclined solar still. *J. Clean. Prod.* **2018**, *172*, 2711–2719. [CrossRef]
29. Manokar, A.M.; Winston, D.P.; Mondol, J.D.; Sathyamurthy, R.; Kabeel, A.E.; Panchal, H. Comparative study of an inclined solar panel basin solar still in passive and active mode. *Sol. Energy* **2018**, *169*, 206–216. [CrossRef]
30. Sibie, S.K.; El-Amin, M.F.; Sun, S. Modeling of water generation from air using anhydrous salts. *Energies* **2021**, *14*, 3822. [CrossRef]
31. Thakur, A.K.; Sathyamurthy, R.; Velraj, R.; Saidur, R.; Hwang, J.Y. Augmented performance of solar desalination unit by utilization of nano-silicon coated glass cover for promoting drop-wise condensation. *Desalination* **2021**, *515*, 115191. [CrossRef]
32. Zanganeh, P.; Goharrizi, A.S.; Ayatollahi, S.; Feilizadeh, M.; Dashti, H. Efficiency improvement of solar stills through wettability alteration of the condensation surface: An experimental study. *Appl. Energy* **2020**, *268*, 114923. [CrossRef]
33. Tu, Y.; Wang, R.; Zhang, Y.; Wang, J. Progress and expectation of atmospheric water harvesting. *Joule* **2018**, *2*, 1452–1475. [CrossRef]
34. Wang, R.; Wang, L.; Wu, J. *Adsorption Refrigeration Technology: Theory and Application*; John Wiley & Sons: New York, NY, USA, 2014.
35. Kaviti, A.K.; Yadav, A.; Shukla, A. Inclined solar still designs: A review. *Renew. Sustain. Energy Rev.* **2016**, *54*, 429–451. [CrossRef]
36. Selvaraj, K.; Natarajan, A. Factors influencing the performance and productivity of solar stills—A review. *Desalination* **2018**, *435*, 181–187. [CrossRef]
37. Kabeel, A.E. Application of sandy bed solar collector system for water extraction from air. *Int. J. Energy Res.* **2006**, *30*, 381–394. [CrossRef]
38. Kabeel, A.E. Water production from air using multi-shelves solar glass pyramid system. *Renew. Energy* **2007**, *32*, 157–172. [CrossRef]
39. Ji, J.G.; Wang, R.Z.; Li, L.X. New composite adsorbent for solar-driven freshwaterproduction from the atmosphere. *Desalination* **2007**, *212*, 176–182. [CrossRef]

40. Hamed, A.M.; Aly, A.A.; Zeidan, E.S. Application of solar energy for recovery of water from atmospheric air in climatic zones of Saudi Arabia. *Nat. Resour.* **2011**, *2*, 8. [CrossRef]
41. Kumar, M.; Yadav, A. Experimental investigation of design parameters of solar glass desiccant box type system for water production from atmospheric air. *J. Renew. Sustain. Energy* **2015**, *7*, 033122. [CrossRef]
42. Kumar, M.; Yadav, A. Composite desiccant material "CaCl2/Vermiculite/Saw wood": A new material for freshwaterproduction from atmospheric air. *Appl. Water Sci.* **2017**, *7*, 2103–2111. [CrossRef]
43. Wang, J.Y.; Wang, R.Z.; Wang, L.W.; Liu, J.Y. A high efficient semi-open system for freshwaterproduction from atmosphere. *Energy* **2017**, *138*, 542–551. [CrossRef]
44. Gad, H.E.; Hamed, A.M.; El-Sharkawy, I.I. Application of a solar desiccant/collector system for water recovery from atmospheric air. *Renew. Energy* **2001**, *22*, 541–556. [CrossRef]
45. Elashmawy, M.; Alshammari, F. Atmospheric water harvesting from low humid regions using tubular solar still powered by a parabolic concentrator system. *J. Clean. Prod.* **2020**, *256*, 120329. [CrossRef]
46. EnergyPlus. Weather Data by Region-Southwest Pacific WMO Region 5—Malaysia; 2021. Available online: https://energyplus.net/weather-region/southwest_pacific_wmo_region_5/MYS (accessed on 10 April 2022).
47. Kumar, A.; Chaudhary, A.; Yadav, A. The regeneration of various solid desiccants by using a parabolic dish collector and adsorption rate: An experimental investigation. *Int. J. Green Energy* **2014**, *11*, 936–953. [CrossRef]
48. IMPAK. Desiccant Chart Comparisons, Sorbent Systems. 2020. Available online: https://bit.ly/3xBT8xY (accessed on 10 April 2022).
49. Tu, Y.D.; Wang, R.Z.; Ge, T.S.; Zheng, X. Comfortable, high-efficiency heat pump with desiccant-coated, water-sorbing heat exchangers. *Sci. Rep.* **2017**, *7*, 40437. [CrossRef] [PubMed]
50. Hanikel, N.; Prévot, M.S.; Fathieh, F.; Kapustin, E.A.; Lyu, H.; Wang, H.; Diercks, N.J.; Glover, T.G.; Yaghi, O.M. Rapid cycling and exceptional yield in a metal-organic framework water harvester. *ACS Cent. Sci.* **2019**, *5*, 1699–1706. [CrossRef] [PubMed]
51. Mitra, S.; Thu, K.; Saha, B.B.; Srinivasan, K.; Dutta, P. Modeling study of two-stage, multi-bed air cooled silica gel+ water adsorption cooling cum desalination system. *Appl. Therm. Eng.* **2017**, *114*, 704–712. [CrossRef]
52. Kabeel, A.E.; Hamed, A.M.; El-Agouz, S.A. Cost analysis of different solar still configurations. *Energy* **2010**, *35*, 2901–2908. [CrossRef]